

## Interpretation of gravity anomalies via terracing method of the profile curvature

Eskandari, M.<sup>1</sup> and Ebrahimzadeh Ardestani, V.<sup>2\*</sup>

1. M.Sc. Graduated, Department of Geophysics, Islamic Azad University of Hamedan, Iran  
2. Professor, Department of Earth Physics, Institute of Geophysics, University of Tehran, Iran

(Received: 12 Dec 2012, Accepted: 20 May 2014)

Research Note

### Abstract

One of the main goals of interpretation of gravity data is to detect location and edges of the anomalies. Edge detection of gravity anomalies is carried out by different methods. Terracing of the data is one of the approaches that help the interpreter to achieve appropriate results of edge detection. This goal becomes a complex task when the gravity anomalies have smooth borders due to gradual change of density contrast. In this article terracing of data has been inspected using the profile curvature method. The synthetic data are used to assess the accuracy and efficiency of the method in edge detection of gravity anomalies. The results of this research have been compared with the results of other methods such as first vertical derivation, analytic signal, tilt angle, horizontal gradient of tilt angle, and laplacian second derivative. Two real data set are also used to show the applicability of the method.

**Keywords:** Analytic signal, Laplacian operator, Local phase angle, Profile curvature.

### 1. Introduction

The anomaly maps of the gravity field do not, in general, represent the boundaries of anomalies clearly, so that most of the existing anomalies are vague and unclear. Various methods have been represented in order to determine anomalies and their boundaries. In this research, one of the newest methods, titled terracing of the potential field using the profile curvature, has been inspected. The terracing operator works iteratively on gravity (using local curvature of the measured fields) to produce a field comprised of uniform domains separated by abrupt domain boundaries (Cordell and McCafferty, 1989). The gravity of the physical field in every domain is fixed for the boundaries. In every point, curvature is calculated by the Laplacian operator. Most of the edge detection methods are actually directional filtering; for example they are arranged in east-west or north-south directions.

The profile curvature method is not limited to specific direction and operates in direction with the most variation of data (Cooper and Cowan, 2009). The terraced map is analogous to a geologic map where domains are separated by the abrupt boundaries. The terracing operation is based

on the fact that a data point belongs only to one domain. A window is moved across the data and the value of the field at the center of the window depending on the curvature of the data is increased, decreased or unchanged (Fig. 1). The consequences of this method on the synthetic data and the real data of Chahbahar zone and Zereshloo's mine have represented the superiority of this method.

### 2. Horizontal and vertical derivatives

Vertical derivative is used extensively in interpretation of potential field anomalies. This filter enhances the details of shallow anomalies. However, as this filter is a high-pass filter, in addition to the surface anomalies, noises will be amplified too. This filter can be used with the first and second orders. However, vertical derivative can be applied with non-integer orders to produce a good equilibrium between signal and noise quantities. This method is preferred when anomaly variation throughout the survey area is uniform. Therefore, the method is appropriate in the areas with different types of data compiling a map with different order of vertical derivatives.

\*Corresponding author:

E-mail: ebrahimz@ut.ac.ir

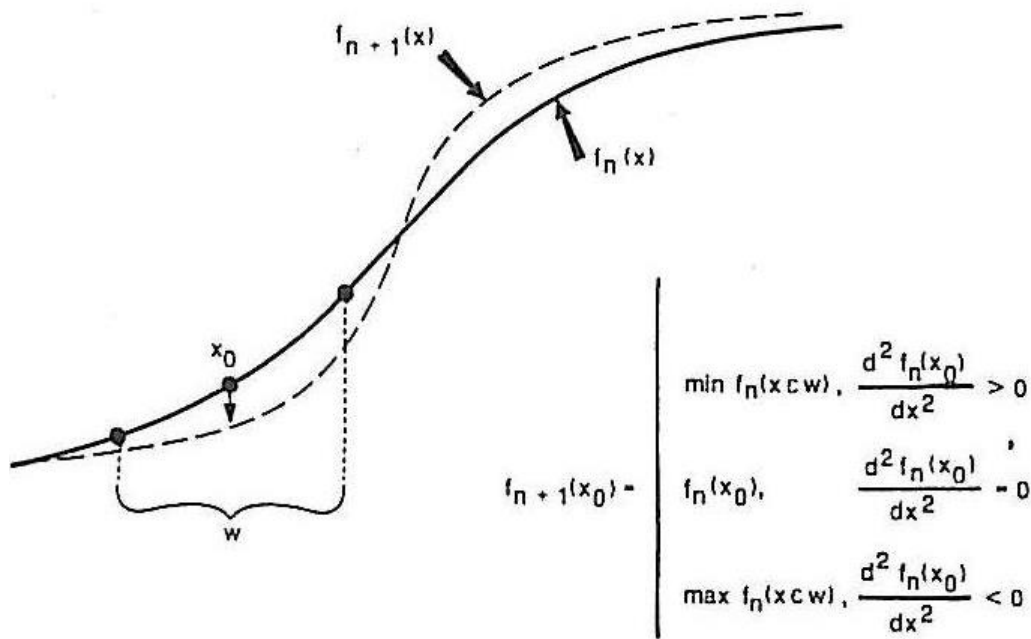


**Fig. 1.** Function values at data point  $x_0$  with  $(n+1)^{th}$  iteration are kept the same or set to the maximum or minimum of  $(n^{th})$  iteration values. This is true within the narrow window  $w$  (centred on  $x_0$ ) on the basis of the direction of the curvature (Cordell and McCafferty, 1989).

The horizontal derivatives enhance the edges; whereas vertical derivatives narrow the width of anomalies, thereby can determine the source bodies more accurately. The higher the order of the derivative used, the more pronounced is the effect. However, as derivative filters are a form of high-pass filter; accordingly, noise in the data is enhanced (Cooper and Cowan, 2004).

The vertical gradient can be computed through following equation (Blakely, 1995):

$$F\left[\left(\frac{\partial^n \varphi}{\partial z^n}\right)\right] = |k|^n F[\varphi] \tag{1}$$

where  $\varphi$  is the gravity anomaly,  $k = 2\pi/\lambda$  and  $F$  is Fourier transform.

**3. Analytic signal operator**

Another popular method to determine the borders is analytic signal. Analytical signal with a simple conversion in a frequency range is an analytical complex operator. The real part and imaginary parts of the analytical signal are horizontal and vertical gradients of gravity data, respectively. Hilbert transform could be used to obtain vertical gradient from horizontal one.

The gravity anomalies or their vertical

gradients (Klingele et al., 1991) are used to compute the analytic signal through following equation:

$$|A_m| = \sqrt{\left(\frac{\partial f}{\partial x}\right)^2 + \left(\frac{\partial f}{\partial y}\right)^2 + \left(\frac{\partial f}{\partial z}\right)^2} \tag{2}$$

where  $f$  is gravity or its vertical gradient.

The analytic signal has a shape on causative bodies that depends on the location of them rather than their amplitudes (Nabighian, 1972). The maximum amount of this area determines anomaly corners on the map.

**4. Tilt angle filters**

Tilt angle is defined by Miller and Singh (1994) as follows:

$$T = \tan^{-1}\left(\frac{\partial f / \partial z}{((\partial f / \partial x)^2 + (\partial f / \partial y)^2)^{0.5}}\right) \tag{3}$$

where  $f$  represents the gravity data. The tilt angle is positive over the source and becomes zero over or near the edge where the vertical derivative is zero and the horizontal derivative is the maximum. It is also negative outside the source region. The tilt angle has a range of -90 to 90 degree and is much simpler to interpret the analytic signal phase angle.

### 5. Horizontal derivative of the tilt angle

Veruzco et al. (2004) suggested use of the total horizontal derivative (THDR) of the tilt angle:

$$THDR = \sqrt{\left(\frac{\partial T}{\partial x}\right)^2 + \left(\frac{\partial T}{\partial y}\right)^2} \quad (4)$$

Pilkington and Keating (2004) showed the reliability and stability of the method for edge detection of magnetic anomalies. This filter was applied for synthetic and real gravity data by Cooper and Cowan (2006).

### 6. Normalized version of the total horizontal derivative

The amplitude of the maximum horizontal gradient enhances edges of any orientation and is given by:

$$fx_{tot} = \sqrt{(\partial f / \partial x)^2 + (\partial f / \partial y)^2} \quad (5)$$

A normalized version of this filter is defined by the following equation (Cooper and Cowan, 2006):

$$TDX = \tan^{-1} \left( \frac{\sqrt{(\partial f / \partial x)^2 + (\partial f / \partial y)^2}}{|\partial f / \partial z|} \right) \quad (6)$$

### 7. Terracing method

Terracing is a method for interpretation of potential field data. Application of this method to the potential field data develops domains in which the measured gravity is constant and their limits by the surroundings are projected by sharp boundaries (Cordell and McCafferty, 1989). Terracing is carried out by calculation of a curvature of 2 and 3 dimensional states. The curve is sharper over the point for which the curvature rate is greater. The curvature of a curve is calculated as follows:

$$k(s) = \left| \frac{d\tau}{ds} \right| \quad (7)$$

where  $\tau$  is the tangent vector of the curve,  $s$  is the length of the curvature and  $k$  is the curvature of the curve. When the data, e.g., the potential field data, have ruptured nature, Laplacian and the profile curvature operator methods have been used for terracing.

#### 7.1. Laplacian operator

The data gradient for one dimensional state using Laplacian derivation is calculated as

follows:

$$L_{1D} = \frac{d^2 f}{dx^2} \quad (8)$$

where  $L_{1D}$  is the curvature in each point. In a moving window (Fig. 1), if the curvature value for the assumed point is zero, the potential field related to the center of the window will remain unchanged. If the estimated curvature value is positive, the potential field related to the center of the window is set the maximum rate, while in case of negative curvature, the potential field is set to the minimum value of the window. Figure 1 shows how the method is applied. The two-dimensional status of the curvature is calculated as follows:

$$L_{2D} = \frac{d^2 f}{dx^2} + \frac{d^2 f}{dy^2} \quad (9)$$

$L_{2D}$  is the curvature point in two dimensional state. This method can be performed repeatedly to reach a better and sharper result.

#### 7.2. Profile curvature method

In this method the curvature of the profile is used. The curvature of the data was computed using directional approximation of the Laplacian operator which is the direction of the steepest ascent at each point of the data. Mathematically, curvature is defined as the change in the slope angle along a very small arc of the curve,  $ds$ , (Fig. 2; Thomas, 1968). Curvature is inverse radius of a circle that is tangent over a small arc over, at least, the three points of the curve (Kepr, 1969). The general equation for curvature ( $k$ ) of a plane section through a point on a surface is (Kepr, 1969):

$$k = \frac{f_x \cos^2 \beta_1 + 2f_{xy} \cos \beta_1 \cos \beta_2 + f_y \cos^2 \beta_2}{\sqrt{q} \cos \phi} \quad (10)$$

where  $\phi$  is the angle between normal vector, on the section plane, and a given point. The  $\beta_1$  and  $\beta_2$  are, respectively, the angles between the tangent of the given normal and the angles between the tangent of a given normal section at a given point and the axes  $x, y$ . where:

$$f_x = \frac{\partial f}{\partial x}, f_y = \frac{\partial f}{\partial y}, f_{xx} = \frac{\partial^2 f}{\partial x^2}, f_{yy} = \frac{\partial^2 f}{\partial y^2}, f_{xy} = \frac{\partial^2 f}{\partial x \partial y}$$

$$p = f_x^2 + f_y^2, q = p + 1$$

For the profile curvature ( $k_s$ ), the value is always in the section plane. The angular relationships are (Mitasova and Jarasalave, 1993):

$$\cos \phi = \sqrt{\frac{p}{q}}, \text{ if } \cos \phi = 1, \cos \beta_1 = \frac{f_x}{\sqrt{pq}}, \cos \beta_2 = \frac{f_y}{\sqrt{pq}}$$

$$k_s = \frac{f_{xx}f_x^2 + 2f_{xy}f_x f_y + f_{yy}f_y^2}{p\sqrt{q^3}} \quad (11)$$

Curvature of the profiles is used in a window analogous to the Laplacian. The movable window on potential field maps would define the separable co-potential areas.

### 8. Synthetic models

The synthetic models are shown in Figure 3a. Figure 3b shows gravity anomalies of the synthetic models. Using the inverse Fourier transform of Equation (1), the edges of the synthetic models are detected and shown in Figure 3c. As it is inspected from the figure, vertical derivatives show the width of anomalies; thereby more accurately we can identify the location of the shallow cubes.

The results of the analytic signal by using Equation (2) have been presented in Figure 2c. The analytic signal is positive over the model,

but the response is blurred due to the model depth.

The results of the tilt angle operation are presented in Figure 3e.

The contour of the theta map also show the location of the model edges, but the response is again blurred due to the model depth.

Figure 3 f shows the result of the THDR operation. Figure 3g shows the normalized total horizontal derivative of the data in Figure 3b. THDR can properly determine shallow sources, while the response from the deeper sources is relatively subdued. TDX, however, can specify both shallow and deep sources.

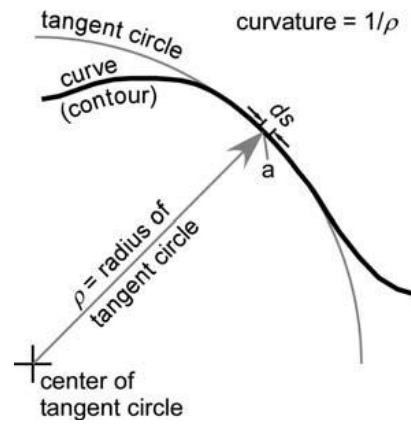


Fig. 2. In a mathematical definition, a curvature is the change in the slope of a curve over a small increment at  $ds$  along the curve at point  $a$ . The curvature is an inverse in the radius of a circle  $\rho$  that is tangent to the curve over the same increment  $ds$  (Thomas 1968).

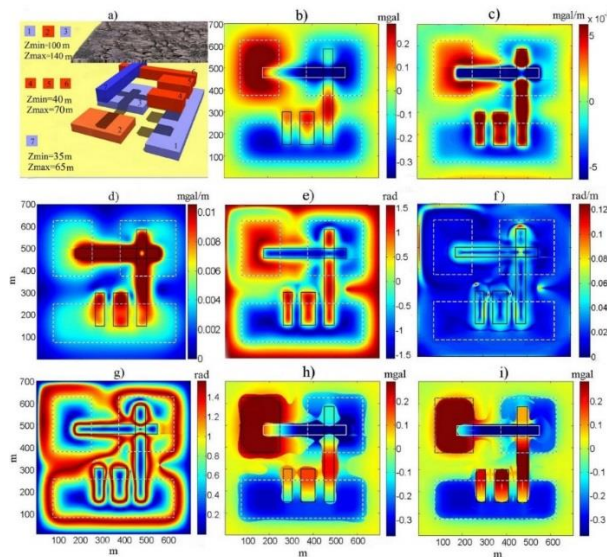
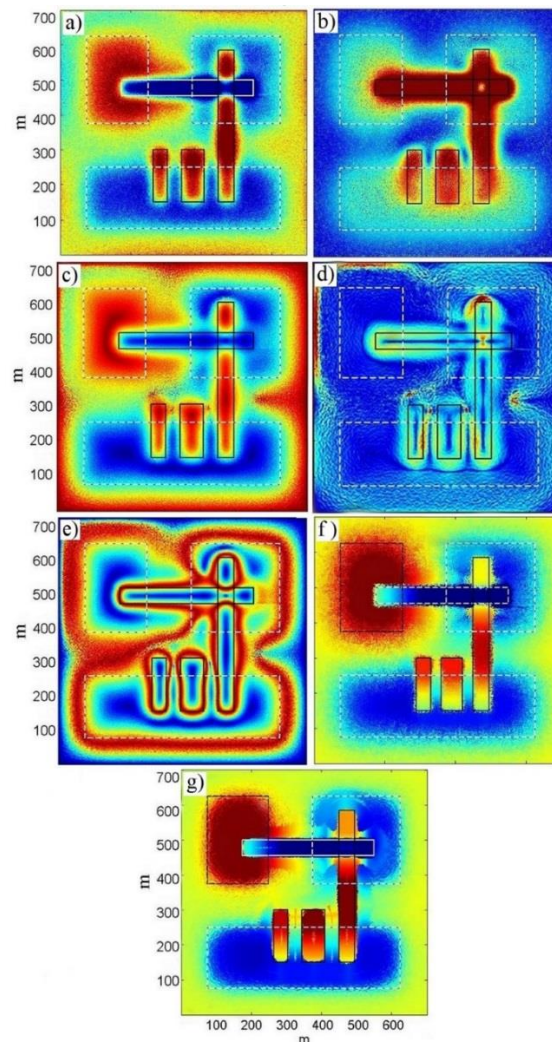


Fig. 3. (a) 3D view of seven rectangular views with different depths. Density contrasts in this figure were  $-1$  and  $1 \text{ g/cm}^3$ , (b) gravity data, (c) the first vertical derivation of data, (d) analytic signal of the data a, (e) tilt angle of the data in a, (f) total horizontal derivative of the tilt angle data (i.e. THDR) using Eq. 3, (g) stabilized amplitude of the total horizontal derivative of the data in a using Eq. 4, (h) the results of the Laplacian derivative function of a, with twenty iterations, (i) the profile curvature function based on the results of a using Eq. 11, with twenty iterations.

Figure 3h shows the results of the Laplacian derivative operation by which the data are segmented into distinct regions centered on each of the seven bodies. The problem of using this method is in its direction of applicability in north-south and east-west.

As it can be seen TDX and THDR filters depicted the borders with high accuracy compared to the analytic signal, Laplacian derivative operator, and the filters based on the local phase. Figure 3i shows the results of the profile curvature operator. The border between cubes shows the high accuracy compared to the vertical derivation, analytic signal, Laplacian derivative operator and the

filters based on the local phase. This method can be performed repeatedly to achieve better and sharper result. Figure 4 shows the gravity data from Figure 3, with a small amount of random noise. According to Figures 3 and 4, it can be revealed that the profile curvature (Fig. 4g) is more robust to noise than the Laplacian function (Fig. 4f), analytic signal operator (Fig. 4b) and the filters based on the local phase. However, as both Laplacian derivative operator and the profile curvature used the second horizontal derivatives of the data, they are prone to noise problems. The data may benefit from smoothing prior to their computation.



**Fig. 4.** (b) Gravity data from Fig. 3d, but a small amount of uniformly distributed random noise is added, (c) gravity data from Fig. 3e, but a small amount of uniformly distributed random noise is added, (d) total horizontal derivative of the tilt angle data (i.e., THDR), but a small amount of uniformly distributed random noise is added, (e) gravity data from Fig. 3g (TDX), but a small amount of uniformly distributed random noise is added., (f) gravity data from Fig. 3h, but a small amount of uniformly distributed random noise is added, (g) gravity data from Fig. 3i, but a small amount of uniformly distributed random noise is added.

## 9. Real data

The consequences of applying the profile curvature method to the two sets of real data are presented here.

### 9.1. First real data set (Chahbahar)

The first real data set belongs to an area close to Chahbahar in southern Iran. The area is shown in Figure 5 (black rectangle).

This area is limited to Jazmoorian in north, Oman Sea in south, Pakistan in east and Zeerdan fault in west. The dominant geological formation of the area is Makran sedimentary basin. The salient characteristic of the Makran sedimentary basin is the existence of east-west oval syncline. This syncline is blocked by the east-west faults.

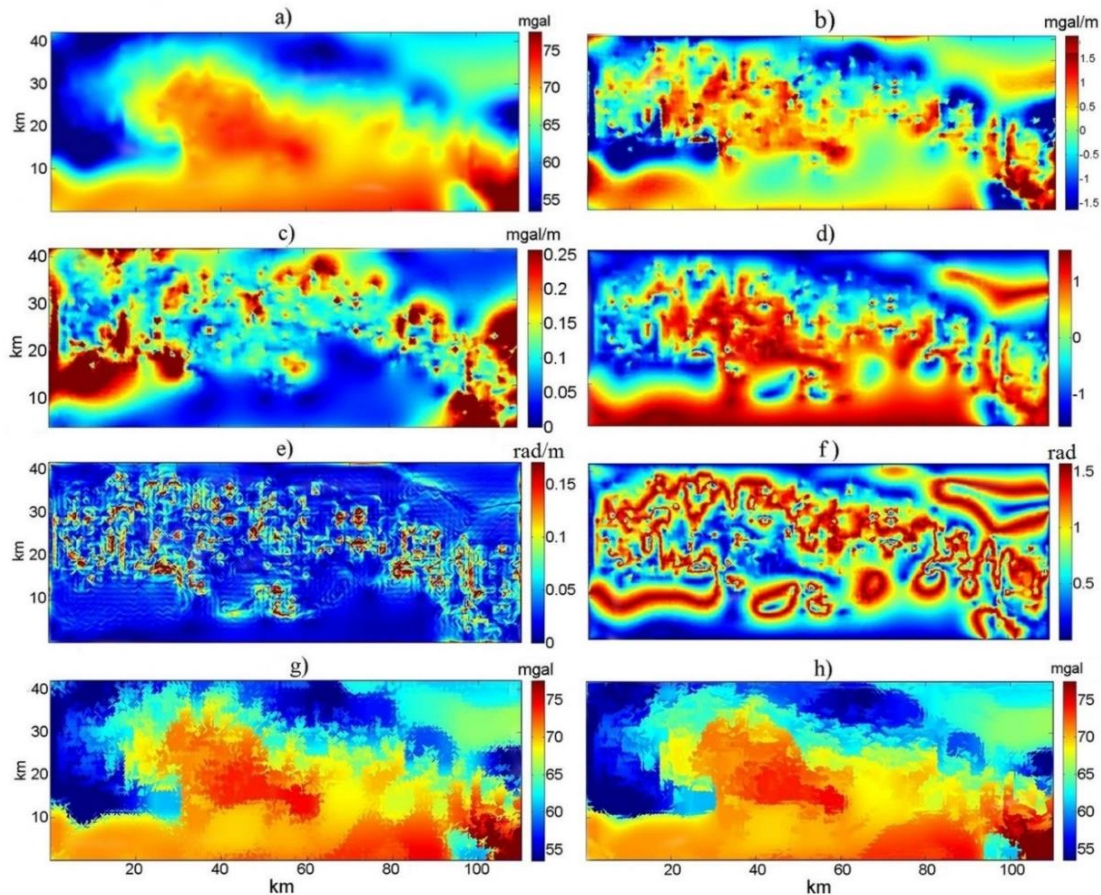
A Scintrex CG3 gravimeter with a sensitivity of 5 micro-Gals is used for reading the data. The altitude of the station was measured by a total station (Leika 506).

Figure 6a shows Bouguer gravity anomalies. Figure 6b shows the first vertical derivatives applied to Bouguer anomalies. Figure 6c shows the analytic signal of the data, with an unclear edges and the figure is cluttered. Figure 6d shows the tilt angle of data in Figure 6a. In Figures 6e and 6f, the total horizontal derivatives (i.e. THDR) of the tilt angle data are compared with TDX (Eq. 6). Figure 6e is dominated by a few large amplitude responses. TDX is also noisy, but shows the smaller features with greater clarity than conventional filters (analytic signal or first vertical derivatives).

Figure 6f shows the total horizontal derivative (TDX) of data in Figure 6a with the stabilized amplitude. Figure 6g shows the gravity data using the Laplacian derivative operator. The ragged behavior of the contours of the terraced data mentioned above is clearly visible throughout the image.



Fig. 5. Map of Iran, Chahbahar and Zereshloo areas are shown with black and red rectangles, respectively



**Fig. 6.** (a) Gravity data from the Bouguer anomaly portion of the Chahbahar, (b) first vertical derivation of a, (c) analytic signal function based on the results of a, (d) tilt angle of the data in a, (e) total horizontal derivative of the tilt angle data (i.e. THDR), (f) stabilized amplitude of the total horizontal derivative of the data in (a), (g) results of the Laplacian derivative function of a, with twenty iterations, (h) profile curvature function based on the results of a, with twenty iterations.

The profile curvature results are shown in Figure 6h. The profile curvature clearly shows the location of some model edges. The most important advantage of terracing methods including profile curvature and Laplacian operator is that they can identify the border of the anomalies without distorting them. On the other hand, the shape of the anomalies, particularly in Bouguer maps, remains unchanged. It should be mentioned that the profile curvature method (Fig. 6h) is quite smoother than the Laplacian operator (Fig. 6g), especially in the border of the anomalies.

## 9.2. Second real data set (Zereshloo)

As a second example, the method was applied to the gravity data of the Zereshloo mine in northern Iran. The location of the mine is shown in Figure 5 with the red rectangle. The main geological structure is Andesite with Iron oxides and Basalt Tuff with Olivine and

Pyroxene. The two are separated by a north-south fault. The complete Bouguer anomalies are shown in Figure 7a. Figure 7b shows the first vertical derivatives of Bouguer anomalies (Fig. 7a). Figure 7c shows the effect of the analytical signal operator. Figure 7d shows the results of tilt angle operator. Figure 7e shows the total horizontal derivatives of the tilt angle results (THDR). Figure 7e shows total horizontal derivative (TDX) with the stabilized amplitude.

The Laplacian and profile curvature results are shown in Figures 7f and 7g, respectively. Boundaries are smoother in Figure 7h than the boundaries in Figure 7g. The advantage explained in section 9.1 is also valid for the obtained results of this set of data. However, as the local anomalies are more dominant in Fig. 7a, Figs. 7b-c shows the edges of these anomalies better than the former set of real data (Figs. 6a-b).

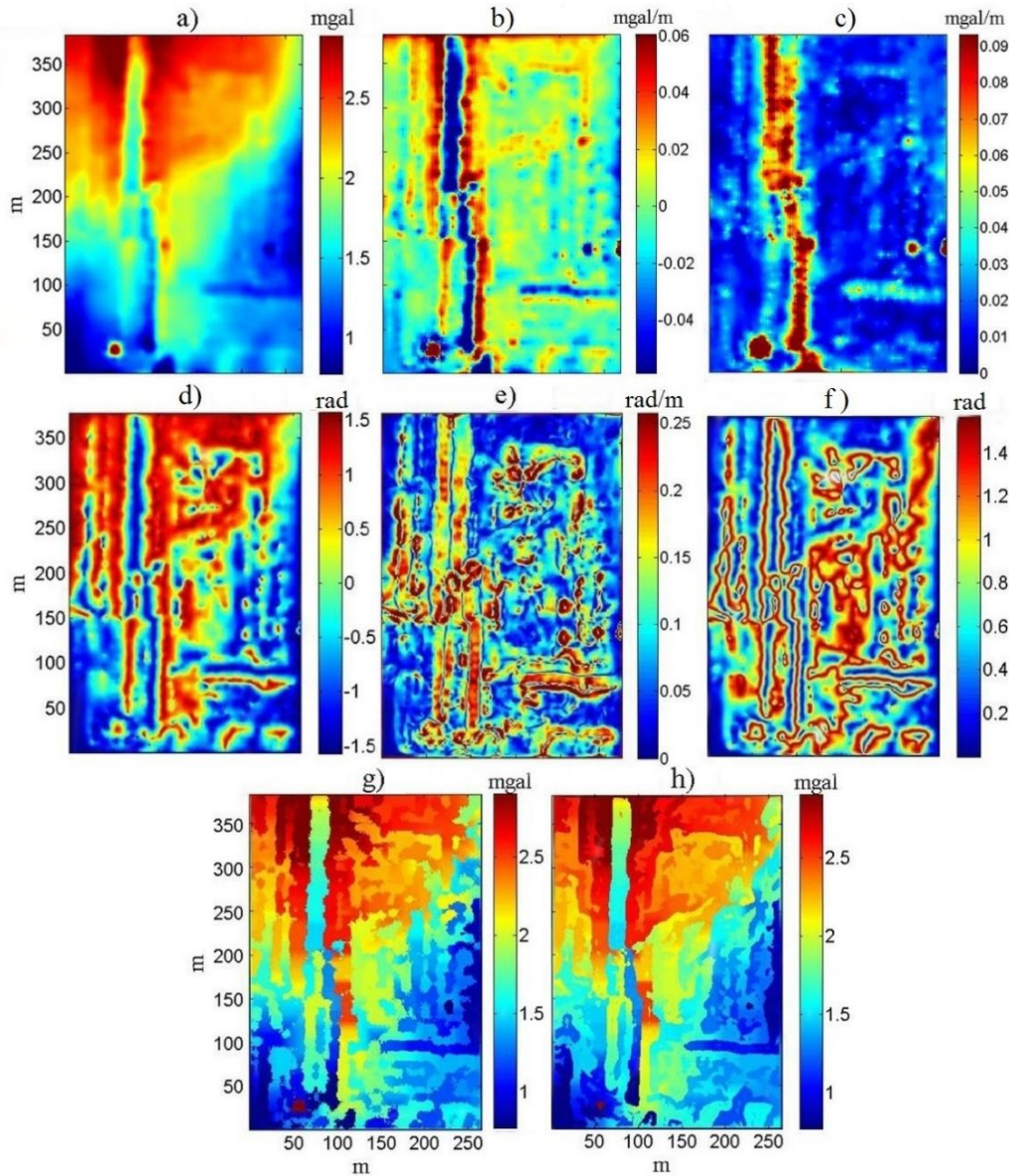


**Fig. 7.** (a) Gravity data from Zereshloo mine in northern Iran, (b) first vertical derivation of a, (c) analytic signal function based on the results of a, (d) tilt angle of data in a, (e) total horizontal derivative of the tilt angle data (i.e. THDR), (f) stabilized amplitude of the total horizontal derivative of the data in a, (g) results of the Laplacian derivative function of a, with twenty iterations, (h) profile curvature function based on the result of a, with twenty iterations.

## 10. Conclusions

Boundary of the gravity anomalies are determined by the following methods: vertical derivation, analytic signal, the filters based on the local phase, and terracing methods. The borders are determined more clearly than the profile of the curvature method. The Laplacian and the profile curvature methods give more accurate results when an iterative process is used. The Laplacian and profile curvature are sensitive to noise, because they help calculate second level format of data. Using the profile

curvature method and the Laplacian operator, the main geology structure is also retained, in addition to specifying the borders. Analytic signal filters and phase angle do not properly represent the effects of deep models, whereas the terracing operator by both methods of Laplacian and profile curvature shows the effect of both deep and shallow models.

## Acknowledgements

The authors are thankful to the Institute of Geophysics, University of Tehran and

Islamic Azad University of Hamedan for all ongoing supports.

### References

- Blakely, R. J., 1995, Potential theory in gravity and magnetic applications, Cambridge University Press, New York 326 pp.
- Cooper, G. R. J. and Cowan, D. R. 2009, Terracing potential field data, *Geophysical prospecting*, 57, 1067-1071.
- Cooper, G. R. J. and Cowan, D. R., 2006, Enhancing potential field data using filters based on the local phase: *Comp. & Geoscience* 32, 1585-1591.
- Cooper, G. R. J. and Cowan, D. R., 2004, Filtering using variable order vertical derivatives, *Computers & Geosciences*, 30, 455-459.
- Cordell, L. and McCafferty, A. E., 1989, A terracing operator for physical property mapping with Potential field data, *Geophysics*, 54, 621-634.
- Kepr, B., 1969, Differential geometry. In: Rektorys, K. (Ed.), *Survey of Applicable Mathematics*, M.I.T. Press, Cambridge, 298-372.
- Klinge, E. E., Marson, I. and Khahle, H. G., 1991, Automatic interpretation of gravity gradiometric data in two dimensions: vertical gradient, *Geophysical Prospecting*, 39, 407-434.
- Miller, H. G. and Singh, V., 1994, Potential field tilt-a new concept for location of potential field sources, *J. Appl. Geophysics*, 32, 213-217.
- Mitasova, H. and Jaroslav, H., 1993, Interpolation by regularized spline with tension: II. Application to terrain modeling and surface geometry analysis, *Mathematical Geology*, 25, 657-669.
- Nabighian, M. N., 1972, The analytical signal of 2D magnetic bodies with polygonal cross-section: Its properties and use for automated anomaly interpretation, *Geophysics*, 37, 507-517.
- Pilkington, M. and Keating, P., 2004, Contact mapping from gridded magnetic data- a comparison: Extended abstracts, ASEG17th Geophysical Conference and Exhibition.
- Thomas, Jr., G. B., 1968, *Calculus and analytic geometry: part two vectors and functions of several variables*, Addison-Wesley Publishing, Reading, MA, USA. 784 pp.
- Veruzco, B., Fairhead, J.D. and Green, C. M., 2004, New insights into magnetic derivatives for structural mapping: *The Leading Edge*, 23(2), 116-119.